Development of a Radiological Characterization Submersible ROV for Use at Fukushima Daiichi

M. Nancekievill, A. R. Jones, M. J. Joyce, *Member, IEEE*, B. Lennox, *Senior Member, IEEE*, S. Watson, *Member, IEEE*, J. Katakura, K. Okumura, S. Kamada, M. Katoh, and K. Nishimura

***Abstract*— To decommission the Fukushima nuclear power plant after the accident caused by a tsunami in 2011, characterization of the fuel debris is required. The precise location and radiological composition of the fuel debris are currently unknown, and the area is submerged making it difficult to investigate the primary containment vessel. An integrated system that includes both radiation detectors and sonar will allow the full localization and characterization of the fuel debris. This paper describes research completed toward the development of a complete system, on-board a low-cost, small form-factor, submersible remotely operated vehicle. A cerium bromide ($CeBr_3$) scintillator detector for dose-rate monitoring and gamma-ray spectrometry has been integrated and validated experimentally with a ^{137}Cs source, both in the laboratory and while submerged. The addition of an Imagenex 831L sonar has enabled technical demonstrations to take place at the National Maritime Research Institute's facility in Japan, where the system was able to characterize the shape and size of synthetic core debris. The combination of geometrical and radiological measurements allows the real-time localization of fuel debris and isotope identification, leading to an invaluable source of information to the workers at Fukushima that will enable increased efficiency and reduce risk during the decommissioning of the site.**

***Index Terms*— Fukushima Daiichi, gamma-ray detection, nuclear decommissioning, radiation monitoring.**

I. Introduction

THE complete characterization of the Fukushima nuclear power plant, after the accident in 2011, is required to enable safe and efficient decommissioning of the site. To achieve this, many systems are being developed to remotely inspect and characterize the internals of the primary containment vessel (PCV) and surrounding suppression chamber [1].

Manuscript received July 16, 2018; accepted July 18, 2018. Date of publication July 23, 2018; date of current version September 14, 2018. This work was supported in part by the Engineering and Physical Sciences Research Council under Grant EPSRC:EP/N017749/1 and in part by the Ministry of Education, Culture, Sports, Science and Technology, Japan. The work of M. J. Joyce was supported by the Royal Society as a Wolfson Research Merit Award Holder.

M. Nancekievill, B. Lennox, and S. Watson are with the School of Electrical and Electronic Engineering, University of Manchester, M1 3BB Manchester, U.K. (e-mail: matthew.nancekievill@manchester.ac.uk).

A. R. Jones and M. J. Joyce are with the Department of Engineering, Lancaster University, Lancaster LA1 4YW, U.K.

J. Katakura is with the Department of Nuclear System Safety Engineering, Nagaoka University of Technology, Nagaoka 940-2188, Japan.

K. Okumura is with the Japan Atomic Energy Agency, Iwaki 970-8026, Japan.

S. Kamada, M. Katoh, and K. Nishimura are with the Marine Risk Assessment Department, National Maritime Research Institute, Mitaka 181-0004, Japan.

Color versions of one or more of the figures in this paper are available online at http://ieeexplore.ieee.org.

Digital Object Identifier 10.1109/TNS.2018.2858563

After the tsunami struck, the immediate area was evacuated with the PCVs of units 1, 2, and 3 flooded for moderation and cooling. However, this took time and several explosions occurred causing the expulsion of radioactive material and leading to uncertainty in the precise location of the reactor fuel and associated core materials. It is believed that molten fuel melted through the bottom of the PCV and into the pedestal. This has yet to be confirmed with the possibility that some of the fuel remains in the reactor, or that it has moved sideways to the exterior of the pedestal and PCV.

Although many portions of the site have now been characterized, such as the grating around the PCV by Hitachi's shape-changing robot [2] and the flooded suppression chamber using multiple remotely operated vehicles (ROVs) [3], the state of the bottom of the PCV and pedestal is still largely uncharacterized [4].

The inability to characterize the PCV and pedestal means that there is uncertainty in the expected dose rates, shape, and size of physical debris, on the top of or surrounding the fuel debris, as well as to its isotopic inventory present and its distribution.

Dose-rate levels of 10 $Gy \cdot h^{-1}$ have been recorded outside the PCV [5], with much higher dose rates anticipated within the PCV and closer to the fuel debris. A complete characterization will provide clarification and aid the decommissioning process.

The approach to characterization that is proposed in this paper is to use a combination of visual inspection, acoustic mapping (2-D/3-D reconstructions), and radiation assessment. To deploy the necessary payload of radiation detectors and sonar devices within the PCV, a submersible is required that can accommodate all of the sensors while retaining a small form factor, so that it can be deployed through the relatively small access ports that are available.

The University of Manchester has developed a low-cost ROV called the Aqua Vehicle EXplorer for *In-situ* Sensing (AVEXIS), which was initially designed for deployment in the Sellafield legacy ponds to aid in the characterization in this cluttered environment [6], [7]. Some initial work has also been completed for detector integration and characterization [8].

Improvements have been made to increase the robustness and adaptability of the ROV for the integration of the required sensors and deployment at Fukushima. A live feed video camera is included for visual inspection and to aid navigation, with complete manual control through a neutrally buoyant

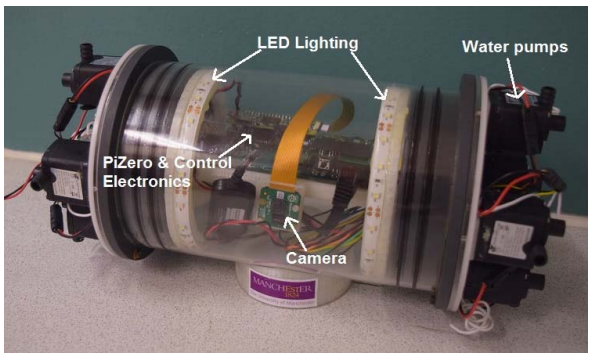

Fig. 1. Photograph of the AVEXIS ROV, adapted from [8].

tether, resistant to entanglement, with a diameter of <10 mm. A sonar system and radiation sensors have also been integrated within the ROV.

This paper presents the experimental validation of the resulting ROV, which contains both a $CeBr_3$ gamma-ray detector and Imagenex 831L sonar [9]. Experiments were conducted in water tanks at Lancaster University, Lancaster, U.K., for the testing of the gamma-ray detector and the National Maritime Research Institute (NMRI), Mitaka, Japan, for the sonar tests.

The remainder of this paper is organized as follows. Section II gives an overview of the ROV and how the design aids the chosen sensors for localization. Section III introduces the integration of the $CeBr_3$ detector and experimental results of the gamma spectrum analysis with a small ^{137}Cs source. Sections IV and V discuss the integration of the sonar used to outline the physical dimensions and shape of the fuel debris. Section VI discusses the results and suggests the options to enable the deployment in the field, and Section VII concludes this paper.

II. Overview of the AVEXIS Submersible ROV

The AVEXIS vehicle, shown in Fig. 1, was designed initially for deployment in the Sellafield legacy fuel storage ponds, to characterize underwater environments which had restricted access [6].

The AVEXIS vehicle consists of a central cylindrical perspex tube that contains all the control electronics, camera, and lighting. It has an outer diameter of 150 mm to enable the deployment through the small access ports. The propulsion system consists of five water pumps located at each end cap which provide three degrees of freedom: forward and backward, up and down, and rotation around the vertical axis.

The turning radius is half the length of the ROV (140 mm), reducing the likelihood of entanglement and increasing the range of environments within which it can be deployed.

The available payload weight of the AVEXIS is approximately 1.5 kg, which is sufficient to accommodate several sensors. Initially, a gamma-ray detector and sonar were integrated within the vehicle, with enough contingency for the later addition of a neutron sensor if required.

An adaptable communication protocol is required to enable high-definition visual inspection, with no delay in image processing, control of the ROV's actuators or outputting of measurements from the detector payloads. It was also desirable

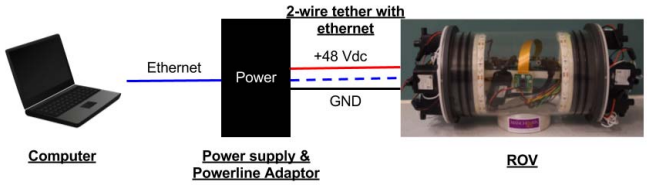

Fig. 2. Schematic of the ROV communication protocol and power through the two-wire tether.

to make the tether as small as possible to reduce the possibility of entanglement and to reduce drag effects on the ROV. This led to the use of an Ethernet-over-power setup, also known as powerline technology, similar to systems used in OpenROV vehicles [10]. Using this technology, transfer speeds of >200 Mb/s can be achieved through a local area network created via a laptop, a powerline adaptor on the surface, and a powerline adaptor in the ROV. The same two wires were used to power the vehicle, as shown in Fig. 2. All detectors attached to the ROV are powered via separate voltage regulators from the main power supply on the surface.

A Raspberry Pi Zero is used for the main control of the ROV and a Raspberry Pi camera is used to return a live video feed with LED strips on the sides of the ROV to aid in visual inspections in poorly lit conditions.

Irradiation tests conducted on some of the constituent components indicated that the total ionizing dose tolerance of the device is greater than 300 Gy(Si). With a target operational lifetime of 10 h, this is considered sufficient, assuming that the dose rate will be approximately 10 $Gy \cdot h^{-1}$.

III. Cerium Bromide Detector Implementation

A. Detector Overview

The gamma-ray detector chosen for deployment within the ROV to characterize Fukushima Daiichi is a $CeBr_3$ inorganic scintillator. $CeBr_3$ is a promising, relatively new scintillation material that has been suggested as one of the best alternatives to replace the more established thallium-doped sodium iodide [NaI(Tl)] [11]–[13]. $CeBr_3$ has the advantage of having a very low intrinsic background radioactivity, unlike other alternatives such as $LaBr_3$ (see [11], [14]) and its energy resolution surpasses that of NaI(Tl) [13]. It also has good pulse linearity [12], [15] and desirable timing properties [15]–[17]. Further advantages of the $CeBr_3$ detector that contributed to its selection as the detection material are: its high detection efficiency, making it ideal for *in-situ* monitoring [14], as well as its radiation robustness to gamma radiation [18].

The detector consists of a 10-mm-diameter crystal coupled with a photomultiplier, connected to an integrated, high-voltage supply unit. This high-voltage unit allows the operation of the detector via a 5-V voltage regulator within the ROV. The detector unit was manufactured by Scionix [19], The Netherlands, and supplied by JCS Ltd., U.K. A schematic of the $CeBr_3$ inorganic scintillator detector is shown in Fig. 3.

B. $CeBr_3$ Gamma Detector Integration

During the initial integration of the $CeBr_3$ gamma-ray detector with the ROV, an RG178 coaxial cable was

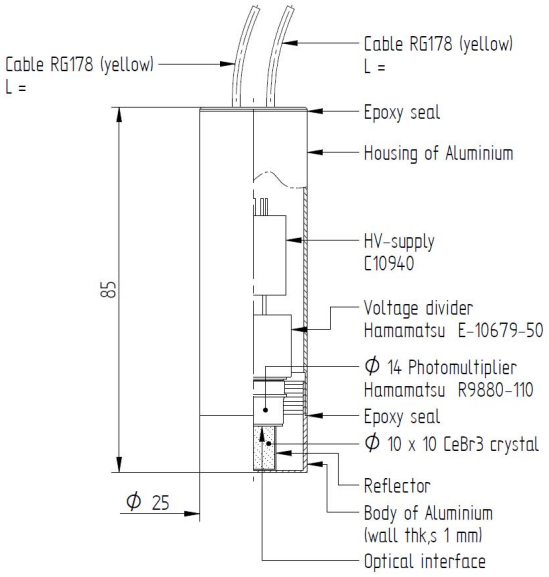

Fig. 3. Dimensional schematic elevation of the $CeBr_3$ inorganic scintillator detector, model VS-0087-50, manufactured by Scionix, The Netherlands [19].

Fig. 4. Photograph of the $CeBr_3$ inorganic scintillation detector, without aluminum casing (left) and with aluminum casing (right), with a U.K. new penny of diameter 20 mm included far left for scale [8].

connected to the signal output from the detector through the ROV. This resulted in two tethers from the ROV; however, the RG178 coaxial cable has a diameter of 2 mm and can be wrapped around the ROV tether. Future iterations of the system will incorporate the coaxial cable within the tether.

As an added layer of protection, the detector was placed in a water-tight aluminum housing inside the ROV to mitigate any unforeseen leaks. The detector can be seen with and without the casing in Fig. 4.

C. Initial Characterization

To determine the impact that the waterproof housing has on the sensitivity of the $CeBr_3$ detector, a set of experiments was undertaken in the laboratory. Two separate sources were used; a 330 kBq ^{137}Cs and a 50 kBq ^{22}Na source. The signal from the detector was passed through and processed by a single-channel, mixed-field analyzer manufactured by Hybrid Instruments Limited, Bailrigg, U.K. [20]. Comparative multichannel analyzer plots from these tests are shown in Figs. 5 and 6.

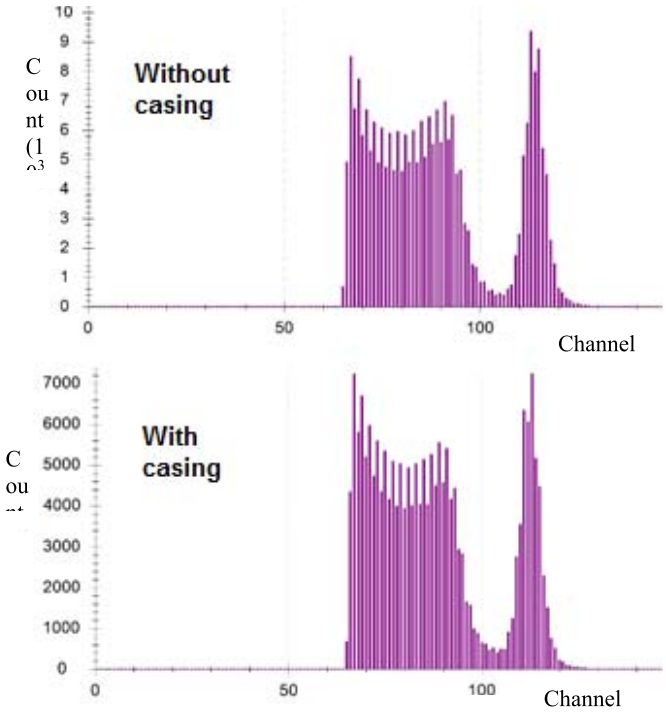

Fig. 5. Energy spectra in terms of counts as a function of channel number for the $CeBr_3$ detector exposed to a ^{137}Cs source for 10 min. The results taken without the casing (top) and the detector within casing (bottom), adapted from [8].

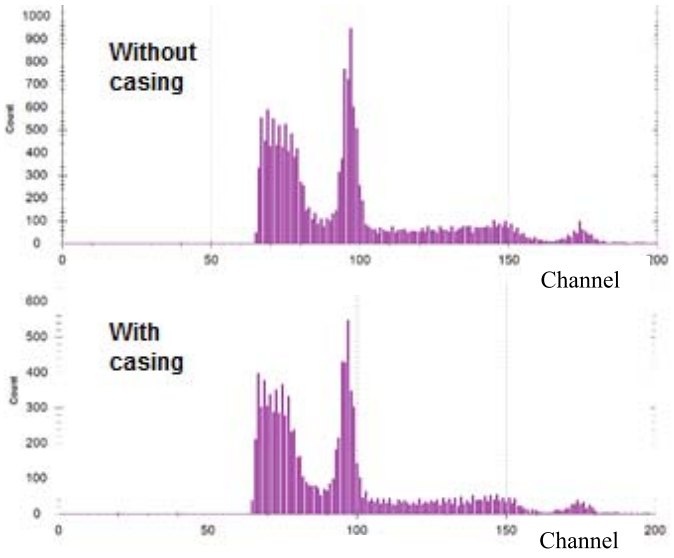

Fig. 6. Energy spectra as in Fig. 5 but for the ^{22}Na source. Results for the detector without casing (top) and those for the detector within casing (bottom), adapted from [8].

Figs. 5 and 6 show that the photopeaks are consistent with one another between the tests conducted with and without the aluminum casings. However, as expected, the relative intensity of the peaks does vary. This is due to the increased distance and shielding effects of the aluminum casing that is located between the detector and source.

A summary of the change in observed throughput of counts during the 10-min experiments, in and out of the casing, can be seen in Table I.

TABLE I
COMPARISON OF NUMBER OF COUNTS WITH AND WITHOUT THE ALUMINUM CASING, ADAPTED FROM [8]

	10 minutes		Pulses per second	
	No Casing	Casing	No Casing	Casing
^{137}Cs source	216291 ±465	174552 ±418	360 ±19	291 ±17
^{22}Na Source	19705 ±140	12485 ±112	33 ±6	21 ±5

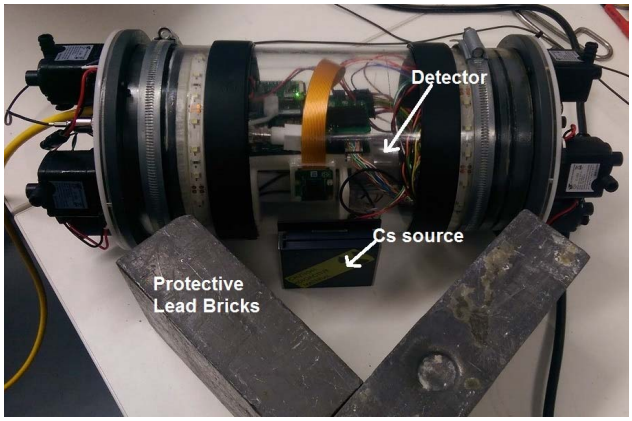

Fig. 7. Photograph of the benchtop test arrangement of the $CeBr_3$ gamma-ray detector integrated within the ROV, adapted from [8].

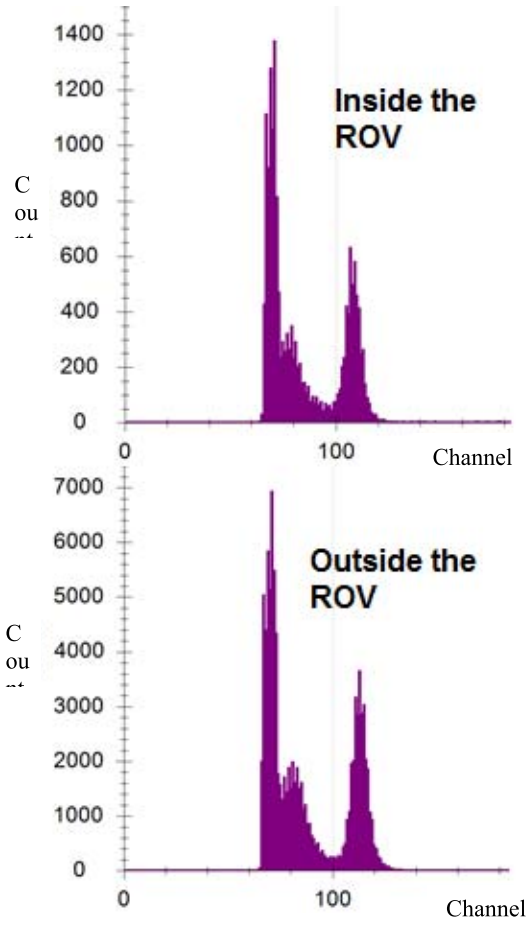

Fig. 8. Spectra of photon counts as a function of channel number for the $CeBr_3$ detector exposed to a ^{137}Cs source for 10 min. Integrated within the ROV (top) and outside the ROV (bottom), adapted from [8].

The results in Table I indicate that the number of counts was reduced by a magnitude of approximately 11–14, when the casing was used. The difference in the magnitude of the attenuation between the two separate sources was assumed to be due to the contrasting energy spectra of these sources. This is expected, with the number of counts for the lower energy spectrum of ^{22}Na, dropping in magnitude by 14× in comparison with 11× for the ^{137}Cs spectrum.

By conducting these experiments, an understanding of the magnitude of count reduction was found to inform the correct measurement of gamma radiation dose rate, while also verifying the expected spectra that would be observed.

D. Integrated ROV Experiments

Having verified the operation of the detector within the aluminum casing, a set of experiments was undertaken to compare the effect of mounting the detector inside and outside of the ROV. These tests were conducted on a laboratory bench top as shown in the photograph in Fig. 7, where the AVEXIS is shown next to the two lead bricks which were used as a precaution to shield the source from the user. In this test, the detector was powered via the main circuitry in the ROV, and the signal was outputted through the RG178 coaxial cable tether.

Fig. 8 shows the response of the detector to a 10-min exposure to a 330 kBq ^{137}Cs source, with the detector located outside the ROV (top) and then inside the ROV (bottom). It can be seen that there are fewer counts when the detector is mounted inside the ROV compared to when it was located outside the ROV. This is due to the increased distance to the source and also, to a lesser extent, the attenuation of the perspex tube of 3-mm thickness. The results suggest that despite this reduction in counts, the detector is still capable of isolating the spectrum of a relatively weak ^{137}Cs source, while operating from within the ROV.

E. Submerged Experiments

A set of experiments was conducted to verify the operation of the $CeBr_3$ detector placed within the ROV while it was submerged. This was to determine the ability of the system to locate radioactive sources underwater, which could then be applied to the decommissioning of Fukushima Daiichi.

Two tests were conducted at Lancaster University's wave tank. The same 330 kBq ^{137}Cs source used in the previous experiments was placed against the internal surface of one of the sides of the wave tank, and the ROV was then placed in the water as close as possible to this source. After this initial verification stage, the ROV was positioned 50 cm away from the side of the tank. The tank wall was made of approximately 10-mm-thick glass. The experimental setup is shown in Fig. 9.

To remain consistent with the previous experiments, two 10-min exposures were taken at each location with the spectra given in Fig. 10.

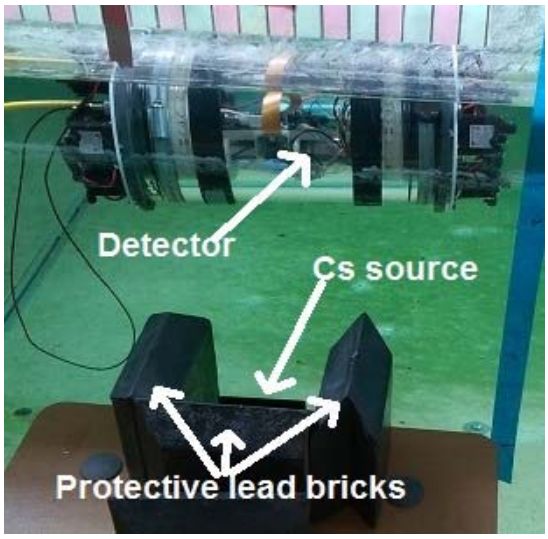

Fig. 9. Photograph of the setup for the submerged ROV gamma-ray detector experiments. The ^{137}Cs source was surrounded by lead bricks and placed up against the side of the tank, with the AVEXIS parallel to the source while submerged, adapted from [8].

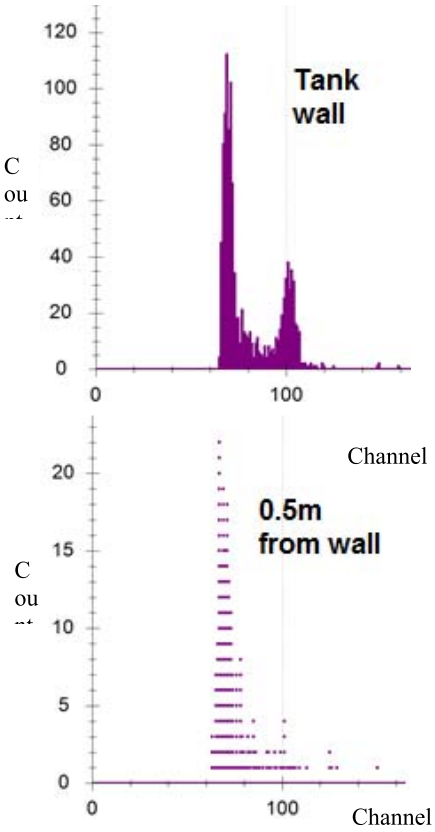

Fig. 10. Spectra of photon counts as a function of channel number for the $CeBr_3$ detector exposed to a ^{137}Cs source for 10 min, while integrated within the ROV and submerged underwater. With the ROV pressed against the side of the tank (top). With the ROV approximately 0.5 m away (bottom), adapted from [8].

It can be seen in Fig. 10 that there is a reduced count in comparison with previous tests due to the increased attenuation caused by the distance and water separating the source and the detector. However, the same structure to the spectra can be seen with the peaks observed as expected. The spectra observed were less defined for the submerged test at 50 cm from the tank side but was still recognisable as a ^{137}Cs source.

This experiment suggests that the detector is capable of characterizing radioactive isotopes through water. A source with increased activity, by definition, would be detected more quickly and would require shorter exposures to return comparable spectra. However, due to health and safety requirements, it is more difficult to replicate this in the laboratory. However, these tests verify the working principle of the $CeBr_3$ gamma-ray detector while integrated within the ROV and submerged.

As the data are outputted in real time, the successful spectral analysis and dose-rate monitoring of the radioactive fuel could enable specific nuclides to be localized within a variety of radioactive material.

As the AVEXIS is adaptable to accommodate the sensors as required by the operator, it is feasible to replace the $CeBr_3$ gamma-ray detector by other detectors, such as a single crystal diamond (made by chemical vapor deposition) neutron detector with a ^{6}Li convertor foil. This could enable the mapping of thermal neutron flux, complementing the gamma-ray detection functionality.

IV. Integration of Sonar Data to Enable Localization of Radioactive Debris

In a cluttered environment such as inside the PCVs at Fukushima Daiichi, knowledge of the physical layout is required to ensure the safe operation of the ROV. Geometric data will also enable the fusion of outputted radiation detector data with a physical map of the reactor, further improving the assessment of the nuclear waste.

The integration of the sonar was supported through collaborators from NMRI, Nagaoka University of Technology, Nagaoka, Japan, and the Japan Atomic Energy Agency, Tomioka, Japan. The objective was to characterize the physical layout of the unknown areas beneath the PCV in the pedestal.

The sonar used was the Imagenex 831L [9], which was chosen due to its design for use in enclosed pipe systems. This requires that the device is small and relatively light, allowing for integration onto an ROV to detect fuel debris. Table II shows the sonar specifications. Table II shows that the communication protocol is Ethernet TCP/IP; therefore, it is possible to use the same powerline technology previously discussed to gather outputted data, removing the need for an additional tether. The sonar was powered from the ROV via the two-wire tether to the surface, and the data were output across the same two wires. This layout can be seen in Fig. 11.

To validate the operation of the sonar, submerged tests were undertaken at a test pond operated by Forth Engineering Ltd., Maryport, U.K. The pond is approximately 8 m wide, 25 m long and 6 m deep, which is representative of a Sellafield legacy pond, while the depth is representative of the PCVs at Fukushima Daiichi.

Fig. 12 shows the output from the sonar. A feature consistent with the corner of the tank can be seen, with the AVEXIS approximately 0.5 m from the tank wall and 0.8 m from the bottom. The two small shapes at the bottom of the tank are drainage hoses with a diameter of 10 cm. This shows the

TABLE II
SPECIFICATIONS OF THE IMAGENEX 831L SONAR

Frequency	2.25 MHz
Transducer	Profiling type, fluid compensated
Transducer Beam Width	1.4° conical
Range Resolution	1/250 of full scale range
Min. Detectable Range	50 mm
Max. Operating Depth	1,000 m
Max. Cable Length	Standard: 100 m CAT5e
Interface	Standard: 10 Mbps Ethernet TCP/IP
Connector	Subconn MCBH-8M-SS
Power Supply	20-32 Vdc at less than 5 W
Dimensions	61 mm dia. X 343 mm length
Weight: In Air In Water	1.2 kg 0.4 kg
Materials	6061-T6 Aluminium & Polyurethane
Finish	Hard Anodize

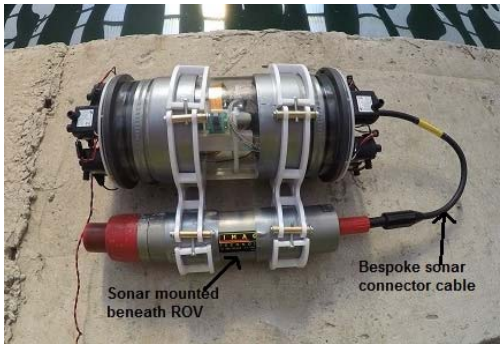

Fig. 11. Photograph of the sonar unit integrated with the ROV.

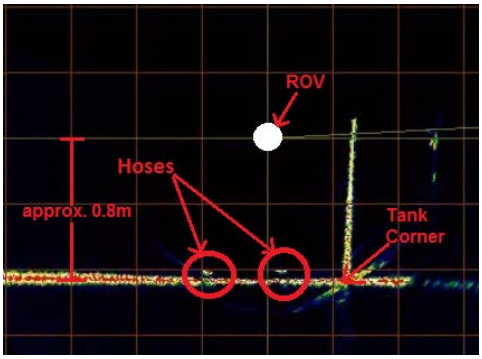

Fig. 12. Example output scan from the sonar unit onboard the ROV in submerged tests with a grid scale of 0.4 m/div, indicating features consistent with the environment, as labeled.

suitability of the system for characterizing debris at the bottom of the PCVs in Fukushima, as broken piping or cylindrical fuel rods are likely debris that will require localization and characterization.

From these tests, it was determined that the sonar data could be retrieved accurately allowing an underwater environment to

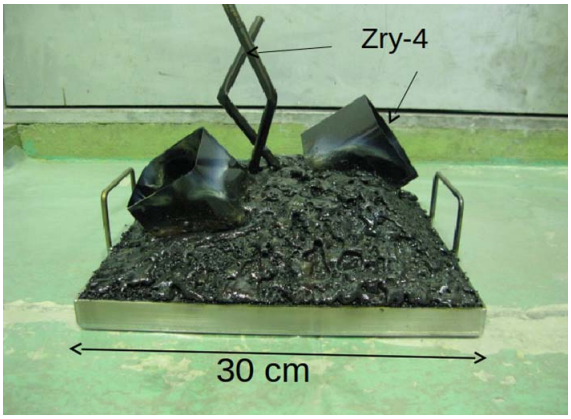

Fig. 13. Photograph of the synthetic debris of the physical form expected to be found at the bottom of the polyvinyl chloride at Fukushima Daiichi.

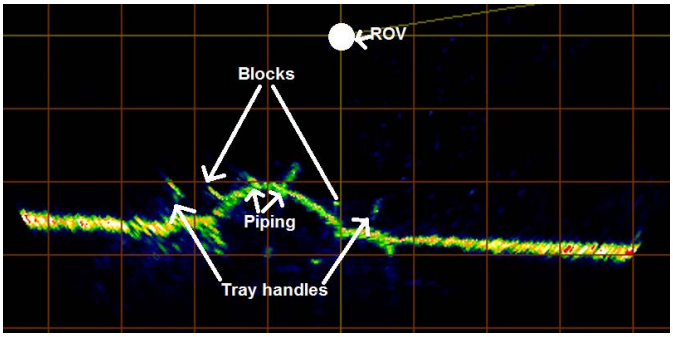

Fig. 14. Output sonar image from tests at the NMRI to characterize synthetic debris.

be characterized in a 2-D plane. To complete a more thorough and representative set of tests to verify the suitability of the sonar to characterize expected radioactive fuel debris, a set of experiments was conducted in Japan.

V. FULLY INTEGRATED EXPERIMENTS

The ROV was taken to a facility operated by Japan's NMRI in Tokyo. This was to determine if both the $CeBr_3$ gamma-ray detector and sonar could be integrated within the ROV at the same time and used to characterize synthetic debris. Radioactive materials could not be placed in the tank, and therefore success for the gamma-ray detector was determined by whether it was able to collect background radiation measurements in real time while the ROV was characterizing the physical shape and size of the debris. The tests illustrated that the detector was able to do this.

To test the sonar's capabilities, synthetic debris was placed at the bottom of the tank. This was representative of what might be expected at Fukushima and is shown in Fig. 13. A layer of sand was placed over this debris to represent sediment that has built up in the PCVs over the course of the last six years. Fig. 14 shows the results of a scan of the simulated debris that was made during the tests. This scan shows a dome representing the debris with the sharp edges of the mock, broken fuel assemblies, and other debris, and provides evidence that the sonar could be used to characterize the debris in the Fukushima Daiichi power plant.

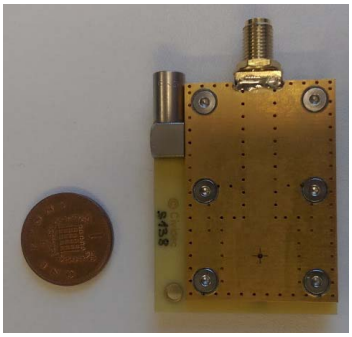

Fig. 15. Photograph of a scCVD diamond neutron detector with a U.K. new penny included for scale.

VI. Discussion

The ability to operate a $CeBr_3$ gamma-ray detector, remotely, while submerged on an ROV has been validated experimentally. While submerged, the $CeBr_3$ gamma-ray detector was able to detect the number of counts over a set time period at different predetermined positions, leading to an approximate source location. Using the approximate location of any source, the ROV could then be positioned so that the detector is exposed to the higher counts required to carry out the more detailed spectral analysis required to identify constituent isotopes. This two-stage analysis could also aid in reducing the radiation damage to the ROV, as proximity to the source would not be reduced (and thus exposure to the radiation not exacerbated) until necessary.

With a source of greater activity, a reduced time of exposure would be required to identify a given radioisotopes to the same extent. In this paper, a duration of 10 min was chosen to confirm the operational abilities of the system with a relatively small source. It is anticipated that isotopic identification will be possible at a much quicker rate, dependent on source activity and ROV distance. In the deployment at Fukushima Daiichi, the level of activity is not expected to be a problem, but, rather, the robustness of the system under high levels of exposure will need to be better understood and the ability to separate important, constituent isotopes from more prominent, and more widely dispersed nuclides.

The integration of a sonar system capable of outputting the physical size and dimension of the internal state of Fukushima Daiichi further aids in the process of localization and characterization of the fuel debris. It could indicate if a source of gamma-ray radiation is likely to be buried beneath other physical debris, and also be used to indicate its location relative to the walls of the PCV. This is critical data for engineers to decommission the site safely and efficiently.

It may also be possible to return a 3-D image of the debris within the reactor using the sonar data and a relative positioning system. This would combine each 2-D plane of sonar data, transforming it into a 3-D model of the reactor. The data received from the $CeBr_3$ gamma detector can then be overlaid onto this image in real time. This would be a valuable source of information for decommissioning engineers.

The ROV has also been designed with adaptability and modularity. The connections and power circuit can also be used to integrate a neutron detector, specifically such as a single-crystal chemical vapor deposition (scCVD) diamond detector. This could be used to provide data about the fuel debris within the Fukushima Daiichi pedestal, which is distinct from ^{137}Cs because cesium is understood to be dispersed widely throughout the water covering the core, the suppression chamber, and surrounding facility; thus, it is not associated uniquely with the debris. The data received from this neutron detector could also be overlaid on a representative 3-D map leading to a greater understanding of the fuel debris situation in Fukushima Daiichi. An example scCVD diamond detector to be integrated in the future is shown in Fig. 15.

Before this device is installed, it will also be necessary to test it in the presence of a significant source of alpha radioactivity and neutrons to be consistent with the Fukushima Daiichi PCV environments.

VII. Conclusion

Integration of a $CeBr_3$ gamma-ray detector into an underwater submersible compatible with the characterizing needs of the inside of the Fukushima Daiichi nuclear power plant has been described. This has been validated experimentally through benchtop and submerged testing, which highlights the reduced counts seen due to attenuation by the ROV and water, while the spectra are still recognizable. Further characterization of the capabilities of this device will be possible with a higher-activity gamma radiation source and multiple submerged sources at specialist facilities.

Integration and experimental validation of a working sonar have been completed to determine the physical location and size of debris inside Fukushima Daiichi. Tests conducted both in the U.K. and Japan outlined the capability of the sonar to physically characterize submerged material consistent with this requirement.

Improvements to both the submersible and gamma-ray spectrometry functions will be conducted with the aim of overlaying positional data of gamma sources in relation to the internal dimensions of the PCV. This will aid the effort to decommission the nuclear power plant and lead to targeted removal of fuel debris, potentially reducing the risk to workers and increasing the efficiency of decommissioning.

References

[1] K. Oikawa, "R&D on robots for the decommissioning of fukushima daiichi NPS," Int. Res. Inst. Nucl. Decommissioning, Tokyo, Japan, Tech. Rep., Feb. 2016.

[2] *Development of a Technology to Investigate Inside the Reactor Primary Containment Vessel (PCV)*, Tokyo Electr. Power, Tokyo, Japan, 2015.

[3] IRID. (2016). *Robots Working Inside the Buildings at Fukushima Daiichi NPS (Part III)*. Accessed: Apr. 16, 2017. [Online]. Available: http://irid.or.jp/en/research/gengorov_trydiver/

[4] *Events and Highlights on the Progress Related to Recovery Operations at Fukushima Daiichi Nuclear Power Station*, IAEA, Vienna, Austria, 2017.

[5] *Development of a Technology to Investigate Inside the Reactor Primary Containment Vessel (PCV)*, Tokyo Electr. Power, Tokyo, Japan, Apr. 2015.

[6] A. Griffiths, A. Dikarev, P. R. Green, B. Lennox, X. Poteau, and S. Watson, "AVEXIS—Aqua vehicle explorer for *in-situ* sensing," *IEEE Robot. Autom. Lett.*, vol. 1, no. 1, pp. 282–287, Jan. 2016.

[7] A. R. Jones *et al.*, "On the design of a remotely-deployed detection system for reactor assessment at Fukushima Daiichi," in *Proc. IEEE Nucl. Sci. Symp.*, Oct. 2016, pp. 1–4.

[8] M. Nancekievill *et al.*, "A remote-operated system to map radiation dose in the Fukushima Daiichi primary containment vessel," in *Proc. EPJ Web Conf.*, vol. 170, 2018, p. 06004.

[9] *IMAGENEX Model 831L Digital Pipe Profiling Sonar*, IMAGENEX, Port Coquitlam, BC, Canada, 2011.

[10] OpenROV. (2017). *OpenROV 2.8 Kit*. Accessed: Apr. 14, 2017. [Online]. Available: https://www.openrov.com/products/openrov28/

[11] E. García-Toraño, B. Caro, V. Peyrés, and M. Mejuto, "Characterization of a $CeBr_3$ detector and application to the measurement of some materials from steelworks," *Nucl. Instrum. Methods Phys. Res. A, Accel. Spectrom. Detect. Assoc. Equip.*, vol. 837, pp. 63–68, Nov. 2016.

[12] K. S. Shah *et al.*, "$CeBr_3$ scintillators for gamma-ray spectroscopy," *IEEE Trans. Nucl. Sci.*, vol. 52, no. 6, pp. 3157–3159, Dec. 2005.

[13] P. Guss, M. Reed, D. Yuan, A. Reed, and S. Mukhopadhyay, "$CeBr_3$ as a room-temperature, high-resolution gamma-ray detector," *Nucl. Instrum. Methods Phys. Res. A, Accel. Spectrom. Detect. Assoc. Equip.*, vol. 608, no. 2, pp. 297–304, 2009.

[14] V. Peyres, T. Crespo, M. Mejuto, and E. García-Toraño, "Measurement of NORM samples with $CeBr_3$ detectors," *Appl. Radiat. Isot.*, vol. 126, pp. 307–310, Aug. 2017.

[15] R. Billnert, S. Oberstedt, E. Andreotti, M. Hult, G. Marissens, and A. Oberstedt, "New information on the characteristics of 1 in.$\times$1 in. cerium bromide scintillation detectors," *Nucl. Instrum. Methods Phys. Res. A, Accel. Spectrom. Detect. Assoc. Equip.*, vol. 647, no. 1, pp. 94–99, 2011.

[16] S. S. Alam *et al.*, "VECC array for nuclear fast timing and angular correlation studies (VENTURE)," *Nucl. Instrum. Methods Phys. Res. A, Accel. Spectrom. Detect. Assoc. Equip.*, vol. 874, pp. 103–112, Dec. 2017.

[17] N. D'Olympia, S. Lakshmi, P. Chowdhury, E. G. Jackson, J. Glodo, and K. Shah, "Sub-nanosecond nuclear half-life and time-of-flight measurements with $CeBr_3$," *Nucl. Instrum. Methods Phys. Res. A, Accel. Spectrom. Detect. Assoc. Equip.*, vol. 728, pp. 31–35, Nov. 2013.

[18] W. Drozdowski, P. Dorenbos, A. J. J. Bos, G. Bizarri, A. Owens, and F. G. A. Quarati, "$CeBr_3$ scintillator development for possible use in space missions," *IEEE Trans. Nucl. Sci.*, vol. 55, no. 3, pp. 1391–1396, Jun. 2008.

[19] SCIONIX. (2017). *SCIONIX*. Accessed: Jun. 2, 2017. [Online]. Available: http://scionix.nl/

[20] Hybrid Instruments. (2016). *Single Channel Mixed-Field Analyser*. Accessed: Jun. 15, 2017. [Online]. Available: http://hybridinstruments.com/products/MFAX1.3.html